Chemistry & Biology, Vol. 12, 835–846, July, 2005, ©2005 Elsevier Ltd All rights reserved. DOI 10.1016/j.chembiol.2005.05.017

Resolving the Profile of Metabolites Generated during Oxidation of Dibenzofuran and Chlorodibenzofurans by the Biphenyl Catabolic Pathway Enzymes

Mahmood Mohammadi and Michel Sylvestre*
Institut National de la Recherche Scientifique
INRS-Institut Armand-Frappier
245 Boulvard Hymus
Pointe-Claire, Québec
H9R 1G6
Canada

Summary

Although the metabolism of dibenzofuran by the biphenyl catabolic enzymes had been inferred in previous reports, the metabolic pattern has never been determined unambiguously. In this work, we describe the evolved biphenyl dioxygenase (BPDO) RR41 that exhibits a higher turnover rate of metabolism toward dibenzofuran and chlorodibenzofurans than the parental *Burkholderia xenovorans* LB400 BPDO. We used RR41 BPDO to identify unambiguously the metabolites produced from the oxygenation of dibenzofuran by LB400 BPDO, and we evaluated their further metabolism by the biphenyl catabolic pathway enzymes of strain LB400. RR41 BPDO was obtained by saturation mutagenesis of targeted amino acid residues. $I^{335}F^{336}N^{338}I^{341}L^{409}$ of LB400 BphA were replaced by $A^{335}M^{336}Q^{338}V^{341}F^{409}$ in RR41 BphA. Data confirm the critical role played by these amino acid residues for substrate specificity and regiospecificity.

Introduction

The first step of most bacterial oxidative catabolic pathways involves a hydroxylation reaction to activate the molecule in order to facilitate further catalytic reactions. Under aerobic conditions, this reaction is often catalyzed by oxygenases that introduce both atoms of molecular oxygen directly on vicinal carbons of the molecule. As an example, biphenyl dioxygenase (BPDO) catalyzes the first step of the four enzymatic step biphenyl catabolic pathway [1] (Figure 1). It also oxygenates a range of biphenyl analogs, including polychlorinated biphenyls (PCBs), dibenzofuran, and dibenzodioxin.

When dibenzofuran is the substrate, two types of dioxygenation reactions can occur depending on its orientation toward the enzyme catalytic center. When the vicinal carbons that are oxygenated comprise one of the two carbons that are bonded to the oxygen atom of dibenzofuran (4a or 5a), the dioxygenation reaction is said to be angular (Figure 1). Angular oxygenation results in a concomitant cleavage of the C-O bond to generate 2,2′,3-trihydroxybiphenyl [2]. When the dioxygenation occurs on vicinal carbons that are not bonded to the oxygen atom of dibenzofuran, the reaction is said to be lateral (as for C1-C-2). Lateral oxygenation can generate three dihydro-dihydroxydibenzofuran isomers.

Several known bacteria can grow on dibenzofuran [2, 3]. These bacteria produce a highly regiospecific dioxygenase that catalyzes only the angular oxygenation of dibenzofuran. The resulting 2,2′,3-trihydroxybiphenyl is then cleaved by a metapyrochatechase to ultimately generate salicylic acid [2, 3]. However, no bacteria able to grow on dibenzofuran through a pathway that involves as a first step a lateral dioxygenation of the substrate has yet been reported. Although lateral oxygenation is not the most desirable mode of attack for dibenzofuran, the fact that several enzymes were reported to effect this reaction, it is important to know the regiospecificity of these enzymes toward dibenzofuran and how the resulting metabolites are further degraded. Among others, the enzymes of the naphthalene and biphenyl catabolic pathways are likely to be involved in the cometabolism of dibenzofuran through a lateral oxygenation [4–8], but the pathway (or pathways) involved has never been elucidated unequivocally. This has an impact on enzyme engineering because it was shown that several evolved enzymes exhibiting enhanced metabolic activity toward chlorobiphenyls were also shown to have increased their turnover rates of lateral oxygenation of dibenzofuran [9]. Therefore, in terms of environmental assessment, it is important to elucidate unambiguously the various metabolic steps that are likely to be involved in the further oxidation of the metabolites generated from lateral dioxygenation of dibenzofuran.

Burkholderia xenovorans strain LB400 [10] (also called *Burkholderia* sp. LB400 [11]) produces one of the best PCB-degrading BPDO of natural origin. BPDO is a three-component enzyme [12–16] (Figure 1). It comprises an iron-sulfur protein (ISP_{BPH}) that catalyzes the addition of molecular oxygen, a flavoprotein reductase (RED_{BPH}) and a ferredoxin (FER_{BPH}) that are involved in the transfer of electrons from NADH to ISP_{BPH}. BPDO components are coded by *bphA* (α-subunit of ISP_{BPH}), *bphE* (β-subunit of ISP_{BPH}), *bphF* (FER_{BPH}), and *bphG* (RED_{BPH}) in *B. xenovorans* strain LB400 [10].

B. xenovorans strain LB400 BPDO oxygenates dibenzofuran inefficiently, principally onto lateral carbons to generate two dihydro-dihydroxydibenzofurans [7, 17] whose structures have not yet been determined unambiguously. 2,2′,3-trihydroxybiphenyl that resulted from angular oxygenation is a minor metabolite [7, 17] of LB400 BPDO. Dibenzofuran is also metabolized by *Pseudomonas* sp. NCIB9816-4 naphthalene dioxygenase (NDO) [8]. The enzyme catalyzes lateral dioxygenation of dibenzofuran to yield 1,2-dihydro-1,2-dihydroxydibenzofuran and 3,4-dihydro-3,4-dihydroxydibenzofuran in a ratio of 61:21. Resnick and Gibson [8] did not report the presence of 2,2′,3-trihydroxybiphenyl among dibenzofuran metabolites generated from this NDO. Becher et al. [4] have shown that biphenyl-induced cells of *Ralstonia* sp. strain SBUG 290 can transform dibenzofuran to a yellow metabolite identified as 2-hydroxy-4-(3′-oxo-3′*H*-benzofuran-2′-yliden)but-2-enoic acid (3′-

*Correspondence: michel.sylvestre@iaf.inrs.ca

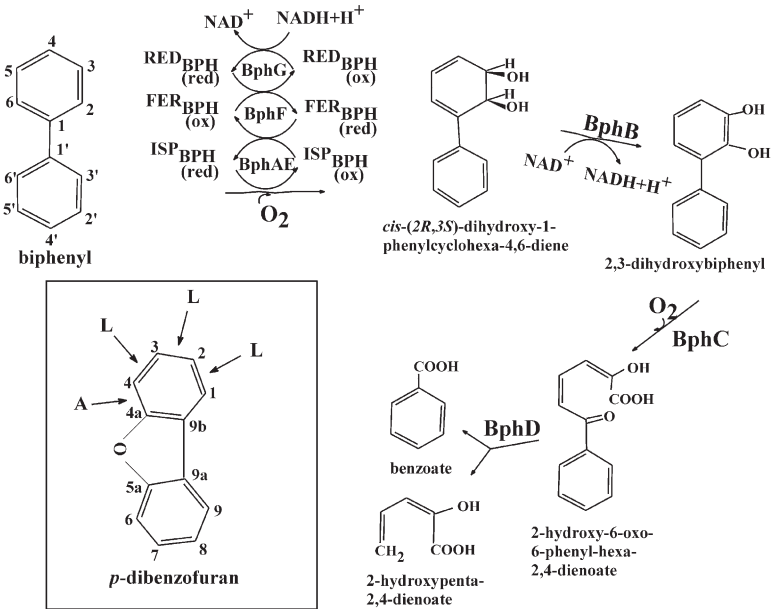

Figure 1. Biphenyl Catabolic Pathway of *B. xenovorans* LB400

The inset shows the structure of dibenzofuran indicating the carbon numbering and the possible oxygenation sites; L indicates lateral, and A indicates angular.

HOBB). This metabolite was presumed to derive from the oxidation of 1,2-dihydro-1,2-dihydroxydibenzofuran followed by the cleavage of 1,2-dihydroxydibenzofuran between carbons 1 and 9b by the biphenyl pathway enzymes [8], but these metabolites were not detected in the growth media. Stope et al. [6] made a similar observation showing that 17 Gram-positive biphenyl-degrading isolates were able to cometabolically transform dibenzofuran to 3′-HOBB during growth on biphenyl. However, because 1,2-dihydroxydibenzofuran was transformed to a yellow metabolite by cells that were not induced by biphenyl [4, 6], the direct involvement of the biphenyl catabolic enzymes in this transformation needed further confirmation. On the other hand, Seeger et al. [7] have shown that incubation of dibenzofuran with an *E. coli* clone expressing *bphAEFGBC* from LB400 produced a yellow metabolite exhibiting a λ_{max} at 464 nm which was presumed to be a *meta*-cleavage compound derived from *cis*-1,2-dihydro-1,2-dihydroxydibenzofuran, but this metabolite was not characterized further. *Pseudomonas putida* G7 harboring plasmid NAH7 [5] that encodes for the naphthalene degrading enzymes [18] was also found to transform dibenzofuran to a *meta*-cleavage metabolite that was identified as *trans*-2-oxo-4-(3′-hydroxybenzofuran-2′-yl)-but-3-enoic acid also called 4-[2′-(3′-hydroxy)-benzofuranyl]-2-keto-3-butenoic acid (3′-HBKB). The metabolic intermediate was presumed to be 1,2-dihydro-1,2-dihydroxydibenzofuran, but it was not detected in the growth medium. Therefore, although the direct participation of the biphenyl or the naphthalene pathway enzymes in the conversion of 1,2-dihydro-1,2-dihydroxydibenzofuran has been inferred from several reports [4, 7], it has never been demonstrated with purified dihydro-dihydroxydibenzofurans and isolated enzymes.

The substrate specificity of BPDO is crucial because it limits the range of compounds potentially degradable by the catabolic pathway [19]. Its regiospecificity is also crucial because it will determine whether the next enzymes of the catabolic pathway can further oxidize the metabolites that are generated from the initial oxygenation of the biphenyl analogs. For example, 2,2′, 5,5′- and 2,2′,3,3′-tetrachlorobiphenyl are oxygenated principally onto vicinal *meta-para* carbons by LB400 BPDO to generate metabolites that cannot be cleaved by 2,3-dihydroxybiphenyl-2,3-dioxygenase (BphC) [20]. Previous reports showed that a stretch of seven amino acids called region III of the C-terminal portion of BPDO α subunit (BphA) strongly influenced the regiospecificity as well as the turnover rate of reaction toward chlorobiphenyls [21, 22]. From random mutagenesis at multiple sites inside region III, we recently obtained variant *p*4 that exhibited a high turnover rate of reaction toward a range of chlorobiphenyls that LB400 BPDO oxygenated poorly [23]. The amino acid sequence of variant *p*4 was identical to that of LB400 BPDO except that $T^{335}F^{336}$ were replaced by $A^{335}M^{336}$. Preliminary data showed that this variant had slightly increased its turnover rate of oxygenation of dibenzofuran compared to LB400 BPDO. On the other hand, residue N^{338} and I^{341} of region III were also found to influence the range of biphenyl analogs that the enzyme can oxygenate [23]. In this work, we screened for new variants exhibiting a higher turnover rate of oxygenation of dibenzofuran than *p*4 BphA from a library of variants obtained by saturation mutagenesis of *p*4 *bphA* at position 338 and 341. Variant RR41 was obtained, and it produced the same metabolites as LB400 BPDO. However, it exhibited a much higher turnover rate of oxygenation of dibenzofuran and chlorodibenzofurans than LB400 BPDO. We used the evolved RR41 BPDO to produce and to identify unambiguously the two dihydro-dihydroxydibenzofurans generated from the oxygenation of dibenzofuran by LB400 BPDO. Furthermore, we have clarified the metabolic profile used by the biphenyl

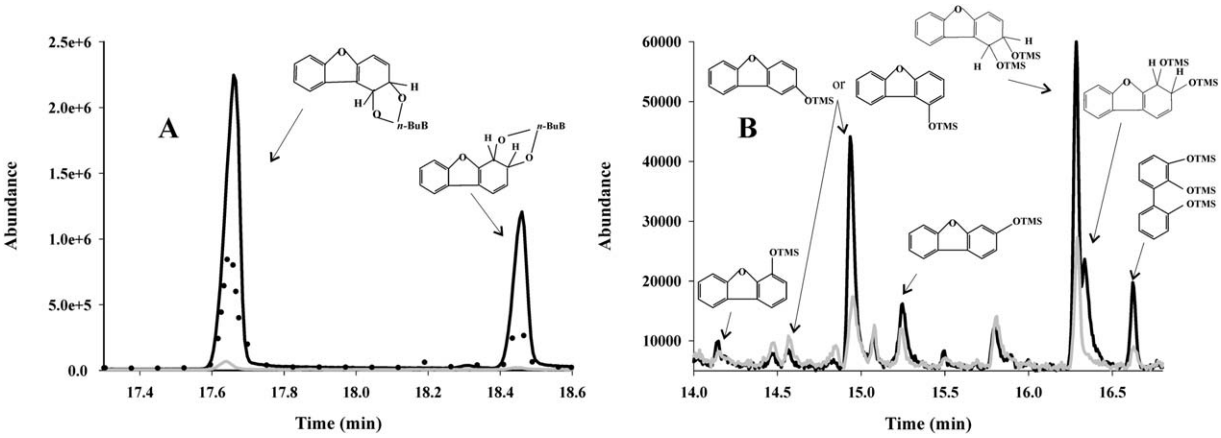

Figure 2. Metabolites Produced from Dibenzofuran by Recombinant *E. coli* Cells Producing Variant BPDOs

Total ion chromatograms of (A) the butylboronate-derived metabolites produced from dibenzofuran by *E. coli* cells expressing LB400 (solid gray line), RR41 (solid black line), or *p*4 (dotted line) BPDO and (B) the TMS-derived metabolites produced from dibenzofuran by His-tagged-purified LB400 (solid gray line) or RR41 (solid black line) BPDO. Induced cell suspensions were incubated with dibenzofuran for 18 hr as described in Experimental Procedures. The enzyme assay set as described in Experimental Procedures was incubated for 5 min at 37°C.

catabolic enzymes to oxidize these two dihydro-dihydroxydibenzofurans.

Results

Isolation of Evolved RR41 BPDO and Its Catalytic Properties toward Dibenzofuran and Chlorodibenzofurans

Saturation mutagenesis at positions N338 and I341 of *p*4 BPDO was performed according to the protocol described in Experimental Procedures. In a library of 60,000 *E. coli* pQE31[bphAE] plus pDB31[bphFGBC] transformants that were exposed to vapors of dibenzofuran, 20 exhibited a deep yellow-orange coloration that suggested a transformation into a *meta*-cleavage metabolite. One of these clones exhibited a clearly more intense yellow-orange coloration than all others; it was designated RR41. Sequence analysis indicated three amino acid substitutions compared to *p4* BphA. They were N338Q, I341V, and L409F.

Resting *E. coli* cells producing LB400 BPDO oxidized 30 nmol of dibenzofuran in 18 hr [17]. Under the same conditions, *E. coli* cells producing variant *p*4 and RR41 BPDOs metabolized respectively 60 nmol and 150 nmol dibenzofuran in 18 hr. Two butylboronate-derived dihydro-dihydroxydibenzofurans (metabolite **1** and metabolite **2**) were detected at a ratio of 95:5 by GC-MS analysis of cultures producing LB400 BPDO [17] (Figure 2A). Cultures producing variant *p*4 and RR41 generated the same two metabolites **1** and **2** at a ratio of 75:25 and 66:33 for variant *p*4 and RR41, respectively (Figure 2A). The relative amount of metabolites **1** and **2** was more difficult to estimate when they were derived with TMS for GC-MS analysis because the dihydro-dihydroxydibenzofurans were transformed to monohydroxydibenzofurans during the analytical procedure (see below). However, TMS derivation permitted the detection in both cultures of 2,2′,3-trihydroxybiphenyl that resulted from angular oxygenation of dibenzofuran (Figure 2B).

Interestingly, resting *E. coli* cells producing RR41 BPDO oxidized 45 nmol 2-chlorodibenzofuran and 30 nmol 4-chlorodibenzofuran in 1 hr, whereas under identical conditions, resting cells producing LB400 BPDO oxidized negligible amount of these two compounds. GC-MS analysis of the TMS-derived metabolites showed that catalytic oxygenation of 2-chlorodibenzofuran generated 2,2′,3-trihydroxy-6′-chlorobiphenyl as major metabolite plus two dihydro-dihydroxydibenzofurans (Figure 3A). Only trace amounts of 2,2′,3-trihydroxy-6′-chlorobiphenyl were detected in culture producing LB400 BPDO. Unlike 2-chlorodibenzofuran, 4-chlorodibenzofuran was metabolized by RR41 BPDO to principally one dihydro-dihydroxy-4′-chlorodibenzofuran with trace amounts of 2,2′,3-trihydroxy-4′-chlorobiphenyl (Figure 3B). LB400 BPDO produced only trace amounts of the dihydro-dihydroxy-4′-chlorodibenzofuran. Therefore, the presence of a chlorine atom on the dibenzofuran molecule significantly influences the enzyme's regiospecificity.

The kinetic properties of His-tagged-purified RR41 BPDO were determined from oxygen consumption rates measured at various concentrations of dibenzofuran or 2-chlorodibenzofuran at pH 6.1 and 37°C. When biphenyl was the substrate, the specific activity of the enzyme preparations used for the determination of the catalytic properties was in the range of 70 to 80 nmol min^{-1} · $nmol^{-1}$ BPDO. Under these experimental conditions, the K_m and k_{cat} values were respectively 12.1 μM and 0.66 s^{-1} for dibenzofuran (k_{cat}/K_m = 5 × 10^4 M^{-1} · s^{-1}) and 30.5 μM and 0.28 s^{-1} (k_{cat}/K_m = 9 × 10^3 M^{-1} · s^{-1}) for 2-chlorodibenzofuran. His-tagged-purified preparations of LB400 BPDO that exhibited a specific activity toward biphenyl similar to that of RR41 BPDO were not sufficiently active toward dibenzofuran or chlorodibenzofuran to calculate reliable values for the enzyme kinetic properties. Therefore, the turnover rates of reaction of RR41 BPDO toward these two substrates were considerably higher than those of LB400 BPDO.

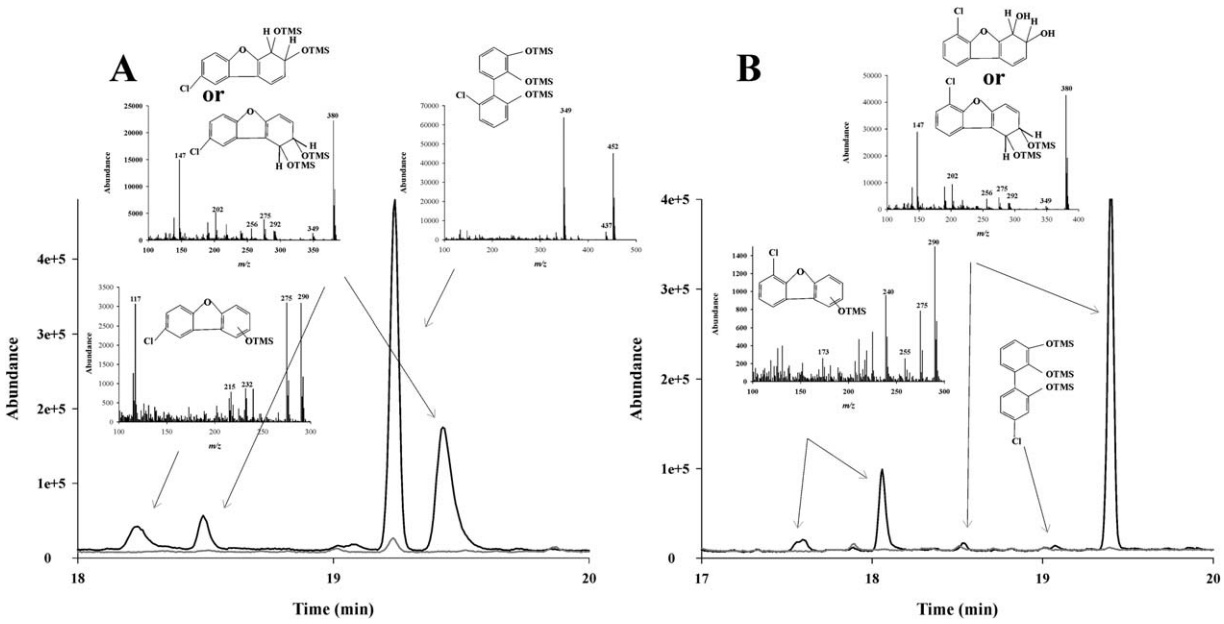

Figure 3. Metabolites Produced from Chlorodibenzofurans by Recombinant *E. coli* Cells Producing Variant BPDOs

Total ion chromatograms of TMS-derived metabolites produced from (A) 2-chlorodibenzofuran and (B) 4-chlorodibenzofuran by *E. coli* cells expressing LB400 (solid gray line) or RR41 (solid black line) BPDO. The mass spectra of the metabolites are also shown in the insets. Two peaks of dihydro-dihydroxy-chlorodibenzofurans exhibiting very similar mass spectral features were detected for each chlorodibenzofuran, but only the spectrum corresponding to the major metabolite is shown. Also note that for matter of clarity, the mass spectrum for 2,2′,3-trihydroxy-4′-chlorobiphenyl is not shown.

Identification of Metabolites 1 and 2

Metabolites **1** and **2** were generated by *E. coli* cells producing variant RR41 BPDO. HPLC-purified metabolite **1** was stable at 20°C in acetonitrile, ethyl acetate, or methanol but the minor metabolite **2** was less stable and was spontaneously converted to 3-hydroxydibenzofuran (see below).

Analysis of the ^{1}H-NMR spectral features identified metabolite **1** as *cis*-1,2-dihydro-1,2-dihydroxydibenzofuran (Figure 4A). The proton assignments were confirmed by proton-proton correlation and heteronuclear multiple quantum correlation (HMQC) experiments that showed that the aromatic proton at C_9 was involved in the Overhauser effect (NOE) observed at H_1. These NMR spectral features were identical to those published for *cis*-1,2-dihydro-1,2-dihydroxydibenzofuran produced by catalytic oxygenation of dibenzofuran by *Pseudomonas* sp. strain 9816-4 NDO [8].

The minor metabolite was unstable. At room temperature, it was rapidly transformed to a monohydroxyl derivative. ^{1}H-NMR analysis of this monohydroxyl compound identified it as 3-hydroxydibenzofuran (Figure 4C). Only aromatic proton signals were detected. The fact that only two protons of the substituted aromatic ring were coupled together showed that the compound could only be 2-hydroxydibenzofuran or 3-hydroxydibenzofuran. Heteronuclear multiple bond correlation (HMBC) and HMQC experiments showed a correlation between the proton H_2 at 6.88 ppm (on C_2) and the carbon C_{9b} at 117 ppm, which confirms the position of H_2 on carbon C_2. Thus, the degradation product of metabolite **2** was 3-hydroxydibenzofuran.

When NMR analysis was performed on a freshly prepared preparation of metabolite **2**, about 25% of the signals detected were from 3-hydroxydibenzofuran. The remaining signals allowed us to identify metabolite **2** as *cis*-3,4-dihydro-3,4-dihydroxy-dibenzofuran (Figure 4B). The two vinyl protons H_1 at 6.62 ppm and H_2 at 5.84 ppm were strongly coupled together, and they were coupled to only one of the methine protons (H_3) at 4.66 ppm. These features give only two possible structures: 1,2-dihydro-1,2-dihydroxydibenzofuran or 3,4-dihydro-3,4-dihydroxydibenzofuran. Because the signals obtained from metabolite **2** in deuterated acetonitrile exhibited chemical displacements and coupling values that differed significantly from the NMR spectra of metablite **1** taken in the same solvant, metabolite **2** was identified as *cis*-3,4-dihydro-3,4-dihydroxydibenzofuran (Figure 4B). These NMR spectral features were identical to those published for *cis*-3,4-dihydro-3,4-dihydroxydibenzofuran produced by catalytic oxygenation of dibenzofuran by *Pseudomonas* sp. strain 9816-4 NDO [8]. *cis*-3,4-dihydro-3,4-dihydroxydibenzofuran was not reported to be unstable by these authors, but its structure was established from NMR analysis of a mixture of *cis*-1,2-dihydro-1,2-dihydroxydibenzofuran and *cis*-3,4-dihydro-3,4-dihydroxydibenzofuran [5].

Both metabolites **1** and **2** were not stable under our condition of TMS derivatization, both of them were transformed to two monohydroxyl derivatives. The major compound obtained from metabolite **2** (accounting for 95% of the total substrate converted) was confirmed by NMR analysis to be 3-hydroxydibenzofuran (not shown). The ratio of the two monohydroxydi-

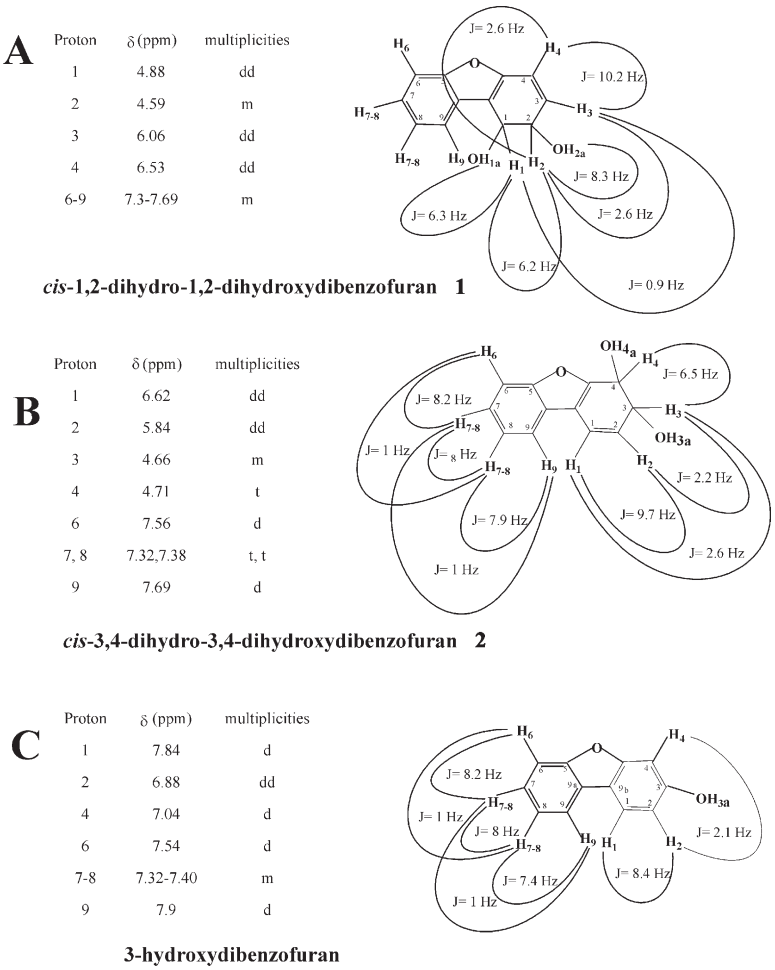

Figure 4. Structural Features of Hydroxylated Metabolites Derived from Catalytic Dioxygenation of Dibenzofuran

Structure of (A) *cis*-1,2-dihydro-1,2-dihydroxydibenzofuran, (B) *cis*-3,4-dihydro-3,4-dihydroxydibenzofuran, (C) 3-hydroxydibenzofuran, and their NMR coupling constants.

benzofuran produced from metabolite **1** was also 95:5. The precise position of the hydroxyl group on these compounds was not determined, but their retention time differed from that of 3-hydroxydibenzofuran and 4-hydroxydibenzofuran produced from *cis*-3,4-dihydro-3,4-dihydroxydibenzofuran (see Figure 2B). However, the proportion of metabolite **1** or **2** that was converted to corresponding monohydroxydibenzofurans was variable, and we were unable to identify the factors (pH, temperature, concentration of dihydro-dihydroxydibenzofuran, etc.) that were responsible for this variation. Nevertheless, the erratic conversion of the dihydro-dihydroxydibenzofurans into monohydroxydibenzofurans during the TMS derivation reaction, indicates that the GC-MS analysis of TMS-derived dibenzofuran metabolites should be used with caution to examine the regiospecificity.

Metabolism of *cis*-1,2-Dihydro-1,2-Dihydoxydibenzofuran and *cis*-3,4-Dihydro-3,4-Dihydroxydibenzofuran

We have used purified His-tagged 2,3-dihydro-2,3-dihydroxybiphenyl-2,3-dehydrogenase (BphB) and BphC to verify their capacity to oxidize the HPLC-purified *cis*-1,2-dihydro-1,2-dihydoxydibenzofuran and *cis*-3,4-dihydro-3,4-dihydroxydibenzofuran. The kinetic properties of BphB toward *cis*-1,2-dihydro-1,2-dihydoxydibenzofuran were calculated at 25°C and at pH 9.0. The K_m value was 72.2 μM and the k_{cat} value was 1.7 s^{-1}. The calculated k_{cat}/K_m value of 2.4×10^4 $M^{-1} \cdot s^{-1}$ is only eight times less than the reported specificity constant of LB400 BphB toward 1,2-dihydroxynaphtalene [24], which is considered to be a good substrate for the enzyme. This shows the effectiveness of BphB to oxidize *cis*-1,2-dihydro-1,2-dihydoxydibenzofuran. When BphB assay was run for less than five min, 1,2-dihydroxydibenzofuran was detected by GC-MS analysis (Figure 5A), but no metabolite was detected when the reaction was prolonged for longer periods. Hammer et al. [25] reported the production of 2,3-dihydroxydibenzofuran from the fungal transformation of dibenzofuran and did not notice that this metabolite was unstable. However, based on its structural similarity with 1,2-dihydroxynaphtalene, it is likely that under our assay conditions, 1,2-dihydroxydibenzofuran was nonenzymatically autooxidized to a quinone derivative [26] that could not be detected by GC-MS analysis. Purified preparations of LB400 His-BphB oxidized *cis*-3,4-dihydro-3,4-dihydroxydibenzofuran to 3,4-dihydroxydibenzofuran that was detected by GC-MS analysis (Figure 5B). Because HPLC-purified *cis*-3,4-dihydro-3,4-dihydroxydibenzofuran was rapidly transformed to 3-hydroxy-

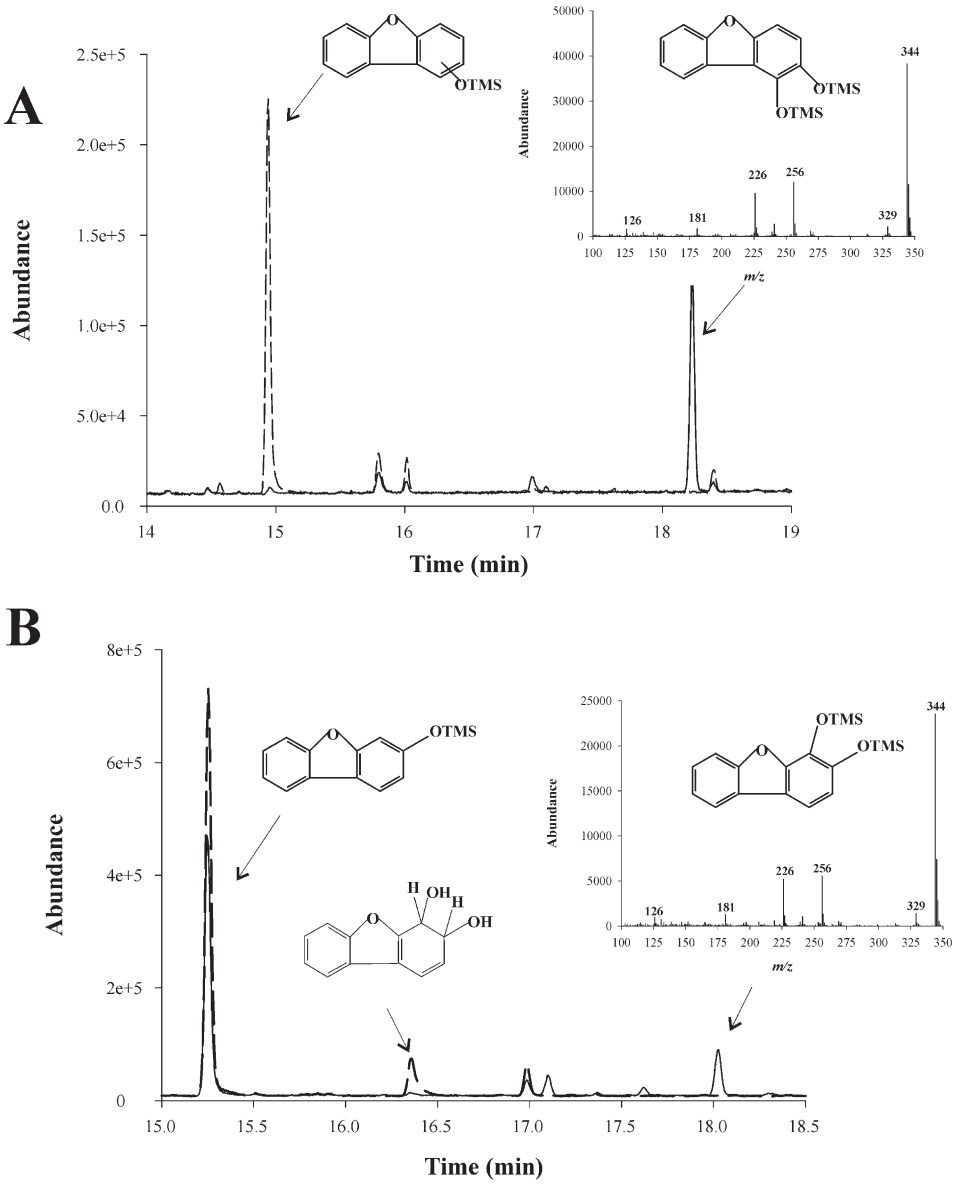

Figure 5. Catalytic Dehydrogenation of Dibenzofuran Metabolites by LB400 BphB

(A) Total ion chromatogram of TMS-derived 1,2-dihydroxydibenzofuran produced from *cis*-1,2-dihydro-1,2-dihydroxydibenzofuran by His-tagged-purified LB400 BphB.

(B) Total ion chromatogram of TMS-derived 3,4-dihydroxydibenzofuran produced from *cis*-3,4-dihydro-3,4-dihydroxydibenzofuran by His-tagged-purified LB400 BphB. Solid line, extract from the reaction vial; dashed line, extract from a control reaction without NAD. The assays were preformed as described in Experimental Procedures. The conversion of the substrate into mono-hydroxydibenzofurans during TMS derivatization was erratic, which explains why *cis*-3,4-dihydro-3,4-dihydroxydibenzofuran was only partially transformed to 3-hydroxydibenzofuran in the control of chromatogram B. The mass spectra of the TMS-derived 1,2-dihydroxydibenzofuran and 3,4-dihydroxydibenzofuran are also shown. Diagnostically important spectral features are: *m/z* = 344 M^+, *m/z* = 329 (M-15), *m/z* = 256 (M-Me_4Si), and *m/z* = 226 (M-Me_4Si-Me_2).

dibenzofuran, it was not possible to use these preparations for establishing the catalytic properties of BphB. However, when approximately 20 nmol of an HPLC-purified preparation of *cis*-3,4-dihydro-3,4-dihydroxydibenzofuran was added to an enzyme assay containing 0.6 nmol His-tagged-purified BphB and 100 nmol NAD, an equivalent amount of NADH was produced after 1 min incubation at 37°C. This suggests that the enzyme oxidized 20 nmol of substrate completely within 1 min of incubation. Similar to 1,2-dihydroxydibenzofuran, 3,4-dihydroxydibenzofuran was also unstable under our enzymatic conditions, and it disappeared rapidly after its formation, suggesting that it was autooxidized to a quinone.

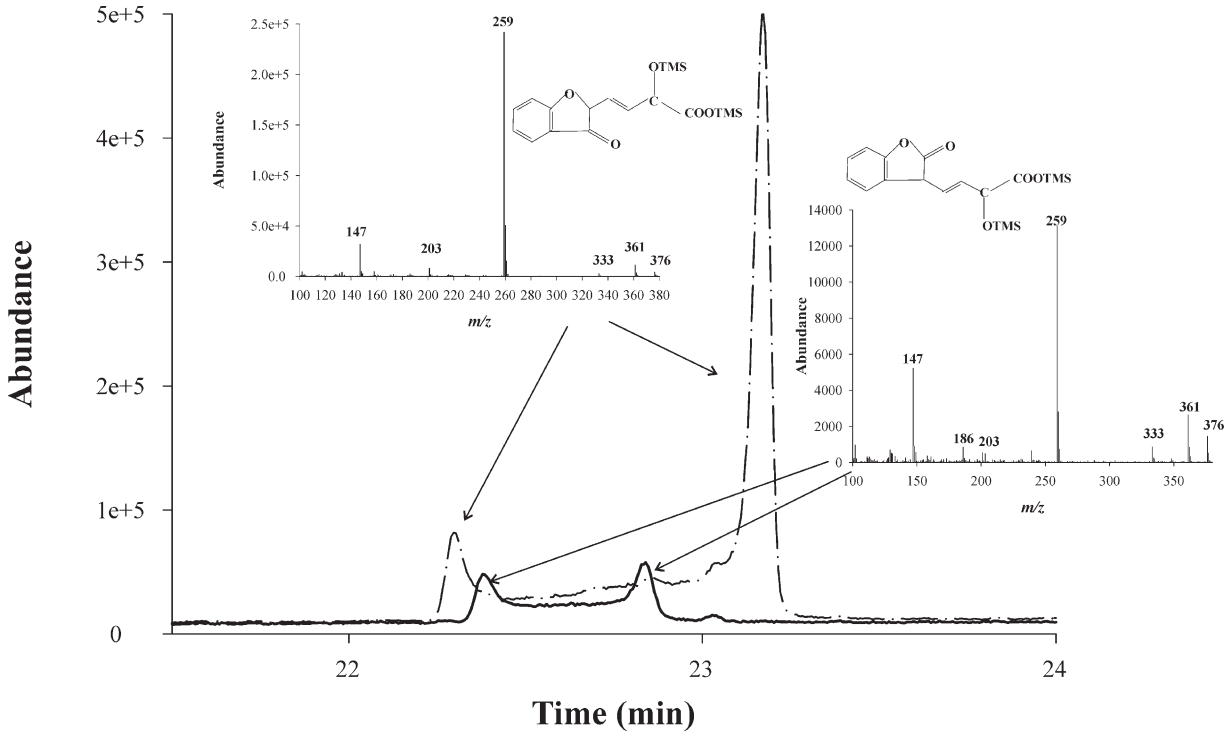

Figure 6. *Meta*-Cleavage Metabolites of Dibenzofuran

The figure shows total ion chromatograms of the *meta*-cleavage metabolites produced from 1,2-dihydroxydibenzofuran by BphC (dashed line) and 3,4-dihydroxydibenzofuran by NahC (solid line) and their mass spectra. The *meta*-cleavage metabolites were produced from the dihydro-dihydroxydibenzofuran by a coupled reaction involving BphB plus BphC or BphB plus NahC as indicated in the text. Only one of the two possible isomers produced from the *meta*-cleavage of 1,2-dihydroxydibenzofuran or 3,4-dihydroxydibenzofuran are shown. Diagnostically important ions are at *m/z* = 376 (M^+), *m/z* = 361 ($M-CH_3$), *m/z* = 333 ($M-CH_3$-CO), and *m/z* = 259 (M-COOTMS).

A coupled reaction involving BphB plus BphC transformed 1,2-dihydro-1,2-dihydroxyxydibenzofuran into a deep yellow-orange metabolite that exhibited a λ_{max} of 462 at pH 7.0. Its λ_{max} shifted from 420 to 462 nm by varying the pH from 3.5 to 7.5. This shift was similar to the one reported for 3′-HOBB [4]. The ring cleavage of 1,2-dihydroxydibenzofuran between C-1 and C-9b can generate two distinct metabolites: 3′-HOBB was the ring-cleavage metabolite produced from dibenzofuran by *Ralstonia* sp. SBUG 290 [4], and 3′-HBKB was the ring-cleavage metabolite produced by *P. putida* G7 [5]. When the yellow metabolite produced from purified BphC was derived with TMS, two peaks, detected by GC-MS analysis (Figure 6), exhibited spectral features characteristic of *meta*-cleavage metabolites reported previously [27, 28]. In these instances, *cis* and *trans* isomers were produced that arose from the rearrangement of the *meta*-cleavage metabolite after the enzymatic reaction [27]. This is supported by Becher et al [4]. NMR data showed that 3′-HOBB spectra exhibited a very diffuse resonance of the methylene protons, indicating that the metabolite isomerized after the enzyme reaction. Data do not permit the unambiguous identification of the *meta*-cleavage metabolite. It could either be *cis-trans* isomers of 3′-HBKB or 3′-HOBB. Nevertheless, the presence of a fragmentation ion at *m/z* = 333 ($M-CH_3$-CO) (Figure 6) is a characteristic feature of a number of α-monohydroxy acid TMS derivatives [27], suggesting that the metabolite is more likely the 3′-HOBB.

Together, these data show that the biphenyl degrading enzymes of LB400 can transform dibenzofuran into at least two *meta*-cleavage metabolites. One of which is the 2-hydroxy-6-oxo-6-[2′-hydroxybiphenyl]-hexa-2,4-dienoic acid [28] resulting from the cleavage of 2,2′,3-trihydroxybiphenyl (see Figure 7), and the other is most likely 3′-HOBB that derived from the cleavage of 1,2-dihydroxydibenzofuran. On the other hand, when *cis*-3,4-dihydro-3,4-dihydroxydibenzofuran was used in a coupled reaction with BphB and BphC, no *meta*-cleavage metabolite was produced in the reaction medium. However, because variant RR41 was found to produce proportionately much more 3,4-dihydro-3,4-dihydroxydibenzofuran than LB400 BPDO, 3,4-dihydroxydibenzofuran is expected to accumulate in the catalytic process. For this reason, we have verified the capacity of 1,2-dihydroxynaphthalene dioxygenase (NahC) to cleave 3,4-dihydroxydibenzofuran. NahC is a dioxygenase homologous to BphC that is involved in the naphthalene catabolic pathway. When a coupled reaction involving BphB plus NahC was used to catalyze the oxidation of *cis*-3,4-dihydro-3,4-dihydroxydibenzofuran, the substrate was converted into a yellow metabolite whose spectral features exhibited a λ_{max} of 420 nm. However, there was no pronounced pH-dependent shift. GC-MS analysis of its TMS derivative (Figure 6)

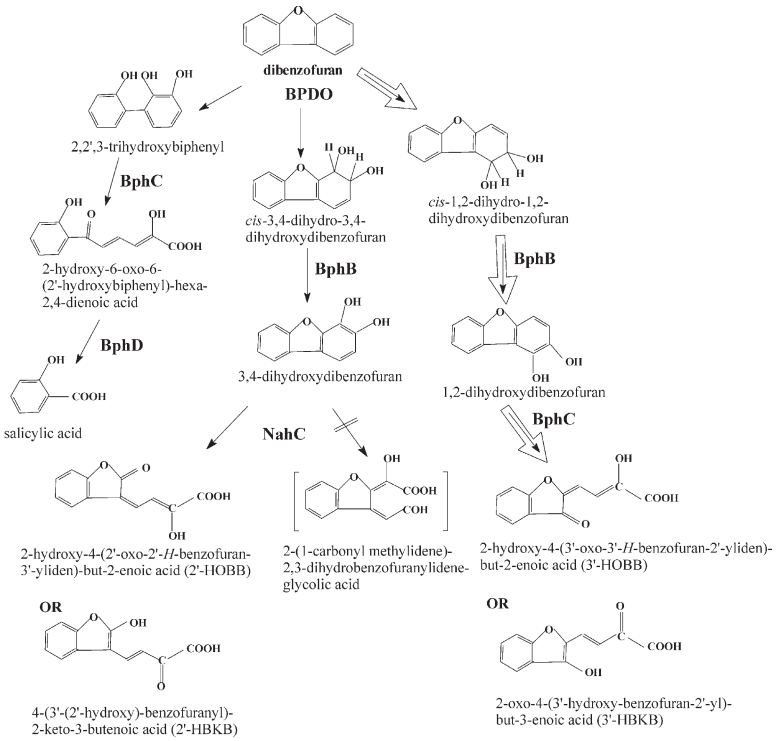

Figure 7. Scheme Showing the Profile of Metabolites Generated during the Oxidation of Dibenzofuran by the Biphenyl Catabolic Enzymes of *B. xenovorans* LB400

Larger arrows show the major metabolic pathway. The scheme also shows the *meta*-cleavage reaction of 3,4-dihydroxydibenzofuran that only NahC can catalyze.

showed two peaks that are likely to represent the *cis* and *trans* isomers of either 2-hydroxy-4-(2′-oxo-2′*H*-benzofuran-3′-yliden)but-2-enoic acid (2′-HOBB) or 4-(3′-(2′-hydroxy)-benzofuranyl)-2-keto-3-butenoic acid (2′-HBKB). These would result from a cleavage between C-4 and C-4a of the 3,4-dihydroxydibenzofuran. A ring cleavage between C-2 and C-3 would have generated 2-(1-carbonyl methylidene)-2,3-dihydrobenzofuranylidene-glycolic acid (CMDFG) (see Figure 7). Based on the mass spectral features of the methyl-derived CMDFG that has been reported [25], the ion fragmentation pattern of its TMS derivative should have included an ion at *m/z* = 244 (M-$CH_3COOTMS$), which is absent from the spectra shown in Figure 6. Similar to above considerations, the presence of a fragmentation ion at *m/z* = 333 (M-CH_3-CO) (Figure 6) suggests that the metabolite is more likely to be the 2′-HOBB. It is worth mentioning that 1,2-dihydro-1,2-dihydroxynaphthalene dehydrogenase, the enzyme homologous to BphB in the naphthalene catabolic pathway can replace BphB in the coupled reaction used to generate HOBB and HBKB from *cis*-1,2-dihydro-1,2-dihydroxydibenzofuran and *cis*-3,4-dihydro-3,4-dihydroxydibenzofuran. Furthermore, NahC can replace BphC to produce HOBB from 1,2-dihydroxydibenzofuran (not shown). Therefore, the enzymes of the naphthalene catabolic pathway metabolize the two dihydro-dihydroxydibenzofurans resulting from lateral oxygenation of dibenzofuran by LB400 BPDO.

Discussion

Sphingomonas sp. HH69 [2] with few other bacteria are able to grow on dibenzofuran. The dioxygenases produced by these strains are highly regiospecific toward the angular carbons of dibenzofuran to generate 2,2′,3-trihydroxybiphenyl, which can be further oxidized to salicylic acid [2]. It is noteworthy that the genes encoding the enzymes involved in dibenzofuran degradation in those strains are scattered on their genome [2, 3, 29]. This might suggests that bacteria have not yet evolved a mature dibenzofuran catabolic pathway comprised of a well-organized operon to control all the genes that were acquired from patchwork assemblages of portions of pathways. Nojiri and Omori [3] pointed out that the length of exposure to dibenzofuran in the environment or the rarity of the genes indispensable for its complete degradation might explain why dibenzofuran catabolic pathways have not yet reach a high level of organization. The same arguments can be used to explain why no bacterial strain able to grow on dibenzofuran through a pathway involving lateral dioxygenation has yet been reported. A better understanding of the enzymatic steps that would be involved in this pathway should help design strategies to construct engineered bacteria able to degrade this persistent pollutant and its chlorinated derivatives more efficiently.

In this work, we investigated the metabolism of dibenzofuran by *B. xenovorans* LB400, which is a natural isolate that can cometabolize this substrate through a pathway involving lateral dioxygenation. Data showed that dioxygenation on the lateral carbons produced *cis*-1,2-dihydro-1,2-dihydroxydibenzofuran as major plus *cis*-3,4-dihydro-3,4-dihydroxydibenzofuran as minor metabolites. Both of these metabolites were oxidized by BphB, the second enzyme of the biphenyl catabolic pathway. However, although BphC cleaved 1,2-dihydroxydibenzofuran, it was unable to cleave 3,4-dihydroxydibenzo-

furan. A more complete oxidation of dibenzofuran by bacteria expressing LB400 BPDO or engineered enzymes derived from it would require an enzyme that can cleave 3,4-dihydroxydibenzofuran. It is interesting that NahC can effect this reaction. Several other examples [20, 30] demonstrated that 1,2-dihydroxynaphthalene dioxygenase is more versatile than BphC to cleave the dihydroxylated metabolites produced from biphenyl analogs. The profile of metabolites generated during the oxidation of dibenzofuran by the enzymes of the biphenyl catabolic pathway is shown in Figure 7. Also shown is the likely catabolic pathway that an engineered bacteria carrying an evolved BPDO effecting lateral dioxygenation of dibenzofuran plus the naphthalene degrading enzyme NahC would follow to oxidize dibenzofuran. It is noteworthy that DoxG (an enzyme homologous to NahC) cleaved 3,4-dihydroxybiphenyl in two ways, either between C-2 and C-3 or between C-4 and C-5 [30]. In this work, NahC cleaved 3,4-dihydroxydibenzofuran in only one way: the cleavage occurred between C-4 and C-4a, which is the position that most closely resembles the cleavage position of 1,2-dihydroxynaphthalene.

Our data showed that the *meta*-cleavage metabolites obtained from 1,2-dihydroxydibenzofuran or 3,4-dihydroxydibenzofuran were not further degraded by the hydrolase of 2-hydroxy-6-oxo-6-phenyl-hexa-2,4-dienoic acid (BphD). Becher et al. [4] showed that salicylic acid was produced from 3′-HOBB by cultures of *Ralstonia* sp. SBUG 290. However, they were unable to show the direct involvement of the biphenyl catabolic enzymes in this transformation. In this context, identifying the enzyme from strain SBUG 290 that oxidized 3′-HOBB to salicylic acid would be of great interest to design engineered bacteria that degrade dibenzofuran efficiently.

It is noteworthy that Selifonov et al. [5] identified 3′-HBKB as the sole *meta*-cleavage metabolite produced from dibenzofuran when *P. putida* G7 cells harboring the naphthalene degrading plasmid NAH7 were used to catalyze its oxidation. 3′-HBKB Should have arisen from the cleavage of 1,2-dihydroxydibenzofuran. Because we found that NahC obtained from NAH7 plasmid can cleave both 1,2-dihydroxydibenzofuran and 3,4-dihydroxydibenzofuran, the data of Selifonov et al. [5] indicate that the NAH7 plasmid-encoded NDO produces only small amounts of 3,4-dihydro-3,4-dihydroxydibenzofuran, if at all. This would be in contrast to the *Pseudomonas* NCIB 9816-4-encoded NDO, which was found to generate a mixture of 1,2- and 3,4-dihydrodihydroxydibenzofuran at a ratio of 61:21 (approximately 3:1) [8]. There is 97% sequence identity between the α subunit of these two NDOs.

Thus, small structural variations of these oxygenases could be responsible for this difference. For example, replacing $T^{335}F^{336}$ of LB400 BphA by $A^{335}M^{336}$ have created a more relaxed variant, *p*4 characterized by an altered regiospecificity toward 2,2′-dichlorobiphenyl [20]. Data suggested that interactions between specific amino acids of BphA and the chlorine substituents of the chlorobiphenyl modulate the orientation that the substrate can take inside the catalytic pocket. Based on the crystal structure of *Rhodococcus* sp. strain RHA1 BPDO [31], residue I^{326} of RHA1 BphA1 that corresponds to F^{336} of LB400 BphA and M^{336} in RR41 BphA makes a direct contact with the biphenyl molecule in the crystal structure of RHA1 BPDO. In this regard, position 335 and 336 of BphA were shown to be critical to determine the orientation of 2,2′-dichlorobiphenyl inside the catalytic pocket. On the other hand, alteration of positions $N^{338}I^{341}$ of *p*4 BphA to $Q^{338}V^{341}$ did not change the regiospecificity of the resulting RR41 variant BphA toward 2,2′-dichlorobiphenyl (not shown). These amino acids do not contact the biphenyl ring in RHA1 BphA1 model. However, the evolved RR41 BPDO exhibited a higher turnover rate of reaction toward dibenzofuran and chlorodibenzofurans than *p*4 and LB400 BPDOs. Similarly, residue 376 of *P. pseudoalcaligenes* KF707 BphA1 (corresponding to 377 of LB400 BphA) was also critical to modulate enzyme activity toward dibenzofuran [9]. Similar to above amino acids, the amino acid corresponding to residue 376 of LB400 BphA does not contact the biphenyl ring in the RHA1 BphA1 model, but its neighbor does. Therefore, regiospecificity can be modulated by amino acid residues other than the ones that interact directly with the biphenyl ring.

Structural analysis of RHA1 BPDO revealed that the two rings of the biphenyl molecule are not coplanar but skewed inside the catalytic pocket of the enzyme [31], each being fixed from both sides through interactions with specific amino acids of the enzyme, one of which being L^{323} of RHA1 BphA1 (L^{333} of LB400 BphA). Dibenzofuran can be regarded as an analog of the symmetrical doubly *ortho* substituted 2,2′-dichlorobiphenyl. However, the bonds between the oxygen atom and the two *ortho* carbons lock both phenyl rings into a coplanar configuration. Therefore, dibenzofuran should position quite differently than biphenyl inside the enzyme catalytic pocket. This might explain why the presence of a single chlorine atom on one of the rings considerably influences the regiospecificity toward these substrates. Thus, RR41 have acquired the capacity to oxygenate 4-chlorodibenzofuran and 2-chlorodibenzofuran more efficiently than the parental enzyme, but the regiospecifity toward these two substrates differed significantly. Nevertheless, it is interesting to point out that 2-chlorodibenzofuran is oxygenated principally onto angular carbons to produce 2,2′,3-trihydroxy-6′-chlorobiphenyl, which should be further transformed to 5-chlorosalicylate by the biphenyl catabolic pathway. This indicates that an engineered bacteria producing RR41 BPDO plus BphB, BphC, and BphD from LB400 would oxidize 2-chlorodibenzofuran to its benzoate intermediate more efficiently than dibenzofuran, which would require the participation of enzymes of other catabolic pathways.

Significance

Aryl hydroxylating dioxygenases are promising enzymes for numerous industrial and environmental applications. These enzymes can be engineered to catalyze the oxygenation of many substrate analogs. Understanding how amino acids of the enzyme catalytic pocket interact with substrate analogs to position them toward the enzyme active center will have

major impacts on the design of strategies to engineer better-performing enzymes. Achieving this goal will require that the identity of the metabolites generated by these engineered enzymes be unambiguously determined. Applying engineered enzymes to environmental processes will also require that we determine unequivocally how the metabolites resulting from catalytic oxygenation of new enzyme substrates are further metabolized by downstream enzymes. In this work, we have investigated the metabolism of dibenzofuran with RR41, an evolved BPDO that oxygenates dibenzofuran and chlorodibenzofurans at much higher turnover rate than the parent *B. xenovorans* LB400 BDO. Several reports dealt with dibenzofuran metabolism by the enzymes involved in the catabolism of biphenyl and naphthalene. However, the metabolism of dibenzofuran by the biphenyl catabolic enzymes has never been established unequivocally. We have purified the metabolites obtained from catalytic oxygenation of dibenzofuran by RR41 BPDO, and we have unambiguously identified them by NMR. The purified compounds were used to verify their metabolism by the enzymes of the biphenyl and naphthalene catabolic pathways. Our data allow proposing an engineered dibenzofuran catabolic pathway based on the biphenyl catabolic enzymes *B. xenovorans* LB400 and the naphthalene catabolic pathway enzymes encoded by plasmid NAH7.

Experimental Procedures

Bacterial Strains, Plasmids, Chemicals, and General Protocols

Escherichia coli DH11S [32], C41(DE3) [33], and XL10-Gold (Stratagene, La Jolla, CA) were used in this study. Plasmids pQE31 [LB400-*bphAE*], pQE31[*p*4-*bphAE*], pDB31[LB400-*bphFG*], pDB31 [LB400-*bphFGBC*], pQE31[NAH7-*nahB*], pQE31[NAH7-*nahC*], and pQE31[LB400-*bphC*] were described previously [15, 21, 23]. To prepare pQE31[LB400-*bphD*], LB400 genomic DNA was PCR amplified with the following two primers: 5′-AGGATCCGACCGCACTCACC GAAAG-3′ and 5′-GACGGTACCTTACGCGTGCCGCAG-3′. The 861 bp BamHI/KpnI DNA fragment was then ligated into the previously BamHI/KpnI-digested pQE31 plamid. pQE31[LB400-*bphD*] was cloned into *E. coli* XL10-Gold. DNA general protocols were done according to Sambrook et al. [34]. DNA was sequenced at the Genome Quebec DNA sequencing center (Montréal, Québec, Canada).

Preparation of DNA, Saturation Mutagenesis, and Screening Protocols to Evolve BphA

The two-step saturation mutagenesis protocol described by Sakamoto et al. [35] was used to simultaneously mutate positions N338 and I341 of variant *p*4 *bphA* except that the two DNA fragments that overlapped inside the *p*4 *bphA* region to be mutated (994–1041 bp) were treated with the Klenow fragment before amplification by PCR. pQE31[*p*4-*bphAE*] DNA was used to mutate *p*4-*bphA.* Primer 1041R (5′-GGGACCACGCGGGTGCCANNNCCGGATNNNGTTCAT AGC-3′) was used in conjunction with primer 1F (5′-CGGGATCCG ATGAGTTCAGCAATCA-3′) to amplify the first 1041 nucleotides of *bphA*. Primer 994F (5′-TTCCTGCCCGCTATGAACNNNATCCGG NNN-3′) was used in conjunction with the reverse primer 2059R (5′-GGTACCCCCTAGAAGAACATGCT-3′) to amplify a 1065 bp DNA fragment that corresponded to the right end portion of *bphA* (starting at 994 bp) plus a portion of *bphE*. The two fragments were combined, assembled with the Klenow fragment, and then amplified by PCR with the antisense oligonucleotides 367F (5′-ACG GCTGGGCCTACGACATC-3′) and 1601R (5′-CTGCGCTTCGCGG TAGTAGAACTGC-3′). The resulting 1234 DNA fragment was digested with MluI and AvrII to generate a library of 864 bp MluI/AvrII fragments that was ligated to pQE31[LB400-*bphAE*] previously deleted from its MluI/AvrII fragment. Expand DNA polymerase (Roche Applied Science) was used. The PCR conditions were set as recommended by the company except that the program was as follows for 35 cycles: 95°C for 45 s, 60°C for 45 s, and 72°C for 1.5 min. The resulting library of plasmids was transformed into *E. coli* DH11S pDB31[LB400-*bphFGBC*] cells, which expressed the entire set of genes required to convert biphenyl into the yellow-colored 2-hydroxy-6-oxo-6-phenylhexa-2,4-dienoic acid. The screening protocol described by Barriault and Sylvestre [23] was used to screen the variants that transformed dibenzofuran into a yellow metabolite. The assumption was made that clones expressing BPDO variants producing higher levels of hydroxylated dibenzofuran metabolites should produce a more intense yellow coloration.

Assays to Identify Dibenzofuran Metabolites and to Quantify the Catalytic Activity of the BPDOs

Assays to identify dibenzofuran metabolites produced by resting cells of *E. coli* were performed according to the protocol described by L'Abbée et al. [17]. IPTG-induced *E. coli* [pDB31*bphFG*] + [pQE31 LB400-*bphAE*], *E. coli* [pDB31*bphFG*] + [pQE31 *p*4-*bphAE*], or *E. coli* [pDB31*bphFG*] + [pQE31 RR41-*bphAE*] were used in these assays. The resting cell suspensions were extracted at neutral pH with ethyl acetate. The ethyl acetate was evaporated under a stream of nitrogen, and the residues were directly used for gas chromatography-mass spectrometry (GC-MS) analysis or they were dissolved in a mixture of water:acetonitrile (80:20 v/v). This solution was injected onto a semipreparative Zorbax-ODS reverse-phase column (9.4 mm by 25 cm). The column was equilibrated with water-acetonitrile (80:20). The compounds were eluted with a linear gradient to water-acetonitrile (20:80) in 20 min at 0.7 ml/min. The Agilent model 1314 variable wavelength detector was set at 307 nm, which was previously determined to be the maximal wavelength of the dihydro-dihydroxydibenzofuran metabolites. Using this system, the two dihydro-dihydroxydibenzofuran metabolites generated from dibenzofuran by *E. coli* [pDB31*bphFG*] + [pQE31 RR41-*bphAE*] eluted as distinct peaks. These peaks were collected, the solvent phase was evaporated in vacuum, and the residual aqueous phase was extracted with ethyl acetate. The identity and purity of the metabolites were confirmed by GC-MS analyses of their butylboronate (*n*BuB) or *N,O-bis*-trimethylsilyl trifluoroacetamide (TMS) derivatives [24, 28]. Nuclear magnetic resonance (NMR) spectra were obtained at the NMR spectrometry center of INRS-Institut Armand-Frappier with a Brucker 500 mHz spectrometer. The analyses were carried out in deuterated acetonitrile at room temperature.

Reconstituted His-tagged-purified BPDO preparations were used in some experiments. The protocol to produce and purify the enzyme components were described previously [20, 21] except that LB400 and RR41 *bphAE* were cloned into pET-14b (Novagen, Madison, WI) and expressed in *E. coli* C41(DE3). The enzyme assays were performed in 50 mM morpholineethanesulfonic (MES) buffer (pH 5.5 or pH 6.1) as described previously [19, 20]. Catalytic activities were determined from measurement of substrate depletion recorded by GC-MS analysis or from measurement of NADH oxidation recorded by fluorometry according to the protocols described previously [19, 36]. The steady-state kinetic parameters of LB400 and RR41 BPDOs were determined by recording the oxygen consumption rates with a Clarke-type Hansatech model DW1 oxygraph [37] for concentrations of dibenzofuran and 2-chlorodibenzofuran varying between 2.5 to 50 μM. The reactions were performed in MES 50 mM (pH 6.1) buffer at 37°C in a volume of 400 μl containing 1.2 nmol of each of the enzyme component and 200 nmol NADH.

Metabolism of 1,2-Dihydro-1,2-Dihydroxydibenzofuran and 3,4-Dihydro-3,4-Dihydroxydibenzofuran by BphB, BphC, and NahC

Purified preparations of *B. xenovorans* LB400 BphB and BphC and *P. putida* G7 NahC were used to assess their ability to metabolize the dihydro-dihydroxydibenzofuran metabolites. The procedures to express these enzymes in recombinant *E. coli* cells and to purify them have been described previously [15, 24]. BphB assays with, as a substrate, HPLC-purified *cis*-1,2-dihydro-1,2-dihydroxydiben-

zofuran or *cis*-3,4-dihydro-3,4-dihydroxydibenzofuran were performed in 500 μl 50 mM MES buffer (pH 7.0) containing 120 nmol NAD. The kinetic parameters (K_m and k_{cat}) were determined for *cis*-1,2-dihydro-1,2-dihydroxydibenzofuran with concentrations between 8 and 120 nM of substrate. The catalytic activity was measured by recording NADH production fluorometrically with an excitation wavelength of 340 nm and an emission wavelength of 453 nm [24]. The metabolites were extracted from the reaction vial with ethyl actetate at neutral pH and derived with *n*BuB or TMS for GC-MS analysis.

The ability of BphC and NahC to oxidize of 1,2-dihydroxydibenzofuran and 3,4-dihydroxydibenzofuran was verified in a coupled reaction with His-tagged-purified BphB. HPLC-purified *cis*-1,2-dihydro-1,2-dihydroxydibenzofuran or *cis*-3,4-dihydro-3,4-dihydroxydibenzofuran were used as substrate. The activity was measured in 50 mM phosphate buffer (pH 7.0) containing 0.6 nmol BphB, 0.6 nmol His-tagged-purified B-356 BphC, or His-tagged-purified G-7 NahC and 100 nmol NAD in a final volume of 500 μl. The enzyme activity was monitored spectrophotometrically at 462 nm for the oxidation of 1,2-dihydroxydibenzofuran and at 420 nm for 3,4-dihydroxydibenzofuran. For GC-MS analysis of the *meta*-cleavage metabolites, the assay medium was acidified to pH 3.5 and extracted with ethyl acetate and treated with TMS for GC-MS analysis.

Acknowledgments

This work was supported by grant number OGP0039579 from the Natural Science and Engineering Research Council of Canada. We thank Nicolas Leberre for assistance in the NMR analyses and his interpretation.

Received: December 22, 2004
Revised: April 15, 2005
Accepted: May 16, 2005
Published: July 22, 2005

References

1. Sylvestre, M. (2004). Genetically modified organisms to remediate polychlorinated biphenyls. Where do we stand? Int. Biodeterior. Biodegration *54*, 153–162.
2. Bressler, D.C., and Fedorak, P.M. (2000). Bacterial metabolism of fluorene, dibenzofuran, dibenzothiophene, and carbazole. Can. J. Microbiol. *46*, 397–409.
3. Nojiri, H., and Omori, T. (2002). Molecular bases of aerobic bacterial degradation of dioxins: involvement of angular dioxygenation. Biosci. Biotechnol. Biochem. *66*, 2001–2016.
4. Becher, D., Specht, M., Hammer, E., Francke, W., and Schauer, F. (2000). Cometabolic degradation of dibenzofuran by biphenyl-cultivated *Ralstonia* sp strain SBUG 290. Appl. Environ. Microbiol. *66*, 4528–4531.
5. Selifonov, S.A., Slepen'kin, A.V., Adanin, V.M., Nefedova, M.I.u., and Starovoitov, I.I. (1991). [Oxidation of dibenzofuran by Pseudomonas strains harboring plasmids of naphthalene degradation]. Mikrobiologiia *60*, 67–71.
6. Stope, M.B., Bacher, D., Hammer, E., and Schauer, F. (2002). Cometabolic ring fission of dibenzofuran by Gram-negative and Gram-positive biphenyl-utilizing bacteria. Appl. Microbiol. Biotechnol. *59*, 62–67.
7. Seeger, M., Camara, B., and Hofer, B. (2001). Dehalogenation, denitration, dehydroxylation, and angular attack on substituted biphenyls and related compounds by a biphenyl dioxygenase. J. Bacteriol. *183*, 3548–3555.
8. Resnick, S.M., and Gibson, D.T. (1996). Regio- and stereospecific oxidation of fluorene, dibenzofuran, and dibenzothiophene by naphthalene dioxygenase from *Pseudomonas* sp strain NCIB 9816-4. Appl. Environ. Microbiol. *62*, 4073–4080.
9. Suenaga, H., Goto, M., and Furukawa, K. (2001). Emergence of multifunctional oxygenase activities by random priming recombination. J. Biol. Chem. *276*, 22500–22506.
10. Erickson, B.D., and Mondello, F.J. (1992). Nucleotide sequencing and transcriptional mapping of the genes encoding biphenyl dioxygenase, a multicomponent polychlorinated-biphenyl-degrading enzyme in *Pseudomonas* strain LB400. J. Bacteriol. *174*, 2903–2912.
11. Denef, V.J., Park, J., Tsoi, T.V., Rouillard, J.M., Zhang, H., Wibbenmeyer, J.A., Verstraete, W., Gulari, E., Hashsham, S.A., and Tiedje, J.M. (2004). Biphenyl and benzoate metabolism in a genomic context: outlining genome-wide metabolic networks in *Burkholderia xenovorans* LB400. Appl. Environ. Microbiol. *70*, 4961–4970.
12. Broadus, R.M., and Haddock, J.D. (1998). Purification and characterization of the NADH:ferredoxinBPH oxidoreductase component of biphenyl 2,3-dioxygenase from *Pseudomonas* sp. strain LB400. Arch. Microbiol. *170*, 106–112.
13. Haddock, J.D., Horton, J.R., and Gibson, D.T. (1995). Dihydroxylation and dechlorination of chlorinated biphenyls by purified biphenyl 2,3-dioxygenase from *Pseudomonas* sp. strain LB400. J. Bacteriol. *177*, 20–26.
14. Haddock, J.D., and Gibson, D.T. (1995). Purification and characterization of the oxygenase component of biphenyl 2,3-dioxygenase from *Pseudomonas* sp. strain LB400. J. Bacteriol. *177*, 5834–5839.
15. Haddock, J.D., Pelletier, D.A., and Gibson, D.T. (1997). Purification and properties of ferredoxin(BPH), a component of biphenyl 2,3-dioxygenase of *Pseudomonas* sp strain LB400. J. Ind. Microbiol. Biotechnol. *19*, 355–359.
16. Hurtubise, Y., Barriault, D., Powlowski, J., and Sylvestre, M. (1995). Purification and characterization of the *Comamonas testosteroni* B-356 biphenyl dioxygenase components. J. Bacteriol. *177*, 6610–6618.
17. L'Abbée, J.B., Barriault, D., and Sylvestre, M. (2005). Metabolism of dibenzofuran and dibenzo-p-dioxin by the biphenyl dioxygenase of Burkholderia xenovorans LB400 and Comamonas testosteroni B-356. Appl. Microbiol. Biotechnol. *67*, 506–514.
18. Yen, K.M., and Gunsalus, I.C. (1982). Plasmid gene organization: naphthalene/salicylate oxidation. Proc. Natl. Acad. Sci. USA *79*, 874–878.
19. Hurtubise, Y., Barriault, D., and Sylvestre, M. (1996). Characterization of active recombinant his-tagged oxygenase component of *Comamonas testosteroni* B-356 biphenyl dioxygenase. J. Biol. Chem. *271*, 8152–8156.
20. Barriault, D., Lepine, F., Mohammadi, M., Milot, S., Leberre, N., and Sylvestre, M. (2004). Revisiting the regiospecificity of *Burkholderia xenovorans* LB400 biphenyl dioxygenase toward 2,2′-dichlorobiphenyl and 2,3,2′,3′-tetrachlorobiphenyl. J. Biol. Chem. *279*, 47489–47496.
21. Barriault, D., Plante, M.M., and Sylvestre, M. (2002). Family shuffling of a targeted *bphA* region to engineer biphenyl dioxygenase. J. Bacteriol. *184*, 3794–3800.
22. Mondello, F.J., Turcich, M.P., Lobos, J.H., and Erickson, B.D. (1997). Identification and modification of biphenyl dioxygenase sequences that determine the specificity of polychlorinated biphenyl degradation. Appl. Environ. Microbiol. *63*, 3096–3103.
23. Barriault, D., and Sylvestre, M. (2004). Evolution of the biphenyl dioxygenase LB400 BphA from *Burkholderia xenovorans* by random mutagenesis of multiple sites in region III. J. Biol. Chem. *279*, 47480–47488.
24. Barriault, D., Vedadi, M., Powlowski, J., and Sylvestre, M. (1999). cis-2,3-dihydro-2,3-dihydroxybiphenyl dehydrogenase and cis-1, 2-dihydro-1,2-dihydroxynaphathalene dehydrogenase catalyze dehydrogenation of the same range of substrates. Biochem. Biophys. Res. Commun. *260*, 181–187.
25. Hammer, E., Krowas, D., Schafer, A., Specht, M., Francke, W., and Schauer, F. (1998). Isolation and characterization of a dibenzofuran-degrading yeast: identification of oxidation and ring cleavage products. Appl. Environ. Microbiol. *64*, 2215–2219.
26. Patel, T.R., and Gibson, D.T. (1974). Purification and properties of (+)-*cis*-naphtalene dihydrodiol dehydrogenase of *Pseudomonas putida*. J. Bacteriol. *119*, 879–888.
27. Massé, R., Messier, F., Ayotte, C., Lévesque, M.-F., and Sylvestre, M. (1989). A Comprehensive gas chromatographic/mass spectrometric analysis of 4-chlorobiphenyl bacterial degradation products. Biomed. Environ. Mass Spectrom. *18*, 27–47.
28. Sondossi, M., Barriault, D., and Sylvestre, M. (2004). Metabo-

lism of 2,2′- and 3,3′-dihydroxybiphenyl by the biphenyl catabolic pathway of *Comamonas testosteroni* B-356. Appl. Environ. Microbiol. *70*, 174–181.

29. Armengaud, J., Happe, B., and Timmis, K.N. (1998). Genetic analysis of dioxin dioxygenase of *Sphingomonas* sp. strain RW1: catabolic genes dispersed on the genome. J. Bacteriol. *180*, 3954–3966.
30. Barriault, D., Durand, J., Maaroufi, H., Eltis, L.D., and Sylvestre, M. (1998). Degradation of polychlorinated biphenyl metabolites by naphthalene-catabolizing enzymes. Appl. Environ. Microbiol. *64*, 4637–4642.
31. Furusawa, Y., Nagarajan, V., Tanokura, M., Masai, E., Fukuda, M., and Senda, T. (2004). Crystal structure of the terminal oxygenase component of biphenyl dioxygenase derived from *Rhodococcus* sp. strain RHA1. J. Mol. Biol. *342*, 1041–1052.
32. Lin, J.J., Smith, M., Jessee, J., and Bloom, F. (1992). DH11s: an *E. coli* strain fro preparation of single-standed DNA from phagemid vectors. Biotechniques *12*, 718–721.
33. Miroux, B., and Walker, J.E. (1996). Over-production of proteins in *Escherichia coli*: mutant hosts that allow synthesis of some membrane proteins and globular proteins at high levels. J. Mol. Biol. *260*, 289–298.
34. Sambrook, J., Fritsch, E.F., and Maniatis, T. (1989). Molecular Cloning: A Laboratory Manual, Second Edition (Cold Spring Harbor, NY: Cold Spring Harbor Laboratory Press).
35. Sakamoto, T., Joern, J.M., Arisawa, A., and Arnold, F.H. (2001). Laboratory evolution of toluene dioxygenase to accept 4-picoline as a substrate. Appl. Environ. Microbiol. *67*, 3882–3887.
36. Hurtubise, Y., Barriault, D., and Sylvestre, M. (1998). Involvement of the terminal oxygenase *beta* subunit in the biphenyl dioxygenase reactivity pattern toward chlorobiphenyls. J. Bacteriol. *180*, 5828–5835.
37. Imbeault, N.Y.R., Powlowski, J.B., Colbert, C.L., Bolin, J.T., and Eltis, L.D. (2000). Steady-state kinetic characterization and crystallization of a polychlorinated biphenyl-transforming dioxygenase. J. Biol. Chem. *275*, 12430–12437.